Journal of Computers Vol. 33 No. 5, October 2022, pp. 135-150
doi: 10.53106/199115992022103305012

Research on Multi-objective Optimization of Freight Train Operation Process Based on Improved Bald Eagle Search Algorithm

Lingzhi Yi[1], Dake Zhang[1*], Wang Li[2], Renzhe Duan[1], Peng Jiang[1], Bo Liu[1]

[1] Hunan Engineering Research Center of Multi-energy Cooperative Control Technology, School of Automation and Electronic Information, Xiangtan University, Xiangtan 411105, China
ylzwyh@xtu.edu.cn, 1912623288@qq.com, 273405269@qq.com, jp_462600@163.com, 337620564@qq.com
[2] CRRC Zhuzhou Electric Motor CO., LTD, Zhuzhou 412001, China
hunanliwang@126.com

Received 5 January 2022; Revised 2 February 2022; Accepted 2 March 2022

Abstract. To study the optimization problem of freight train operation process under complex line conditions, this paper adopts the freight train multi-particle model to establish the multi-objective optimization model of the freight train. Aiming at the problem of difficult optimization caused by complex line conditions, a two-step method is used to find the optimal operation strategy of the freight train. Firstly, the greedy algorithm is used to select the optimal working condition sequence. Secondly, the multi-objective optimization algorithm is used to obtain the position of the ideal working condition transition point. By introducing the idea of non-dominated sorting, an improved multi-objective bald eagle search algorithm is proposed to optimize the operation process of freight trains. This algorithm adopts the evolution method of combining bald eagle population renewal with adaptive Gaussian mutation, and introduces preference information to increase the rationality of population evolution. The simulation results show that the optimal operation strategy of freight train selected by two-step method is in line with the actual operation situation, and the proposed multi-objective bald eagle search algorithm considers both convergence and distribution. The results can satisfy the preference of decision-makers, which can provide a reference target speed curve for railway workers.

Keywords: freight train, multi-particle model, multi-objective optimization, bald eagle search algorithm, preference information, target speed curve

1 Introduction

With the rapid development of the transportation network, freight trains, with their advantages of large volume, fast speed, low cost and all-weather, gradually incline the freight transportation to railway freight transportation [1]. Therefore, more and more attention has been paid to the energy-saving and optimization of freight train operation. Under the conditions of complex lines, the operation process of freight trains should not only consider the balance of energy consumption and time, but also consider the speed limit, decoupling and other safety issues, which is essentially a multi-objective, multi-constraint optimization problem. In order to find a satisfactory operation strategy among many operation strategies, and ensure energy saving, time saving, and safe and stable operation of freight trains, it is of great significance to optimize the operation process of freight trains.

For the energy-saving operation strategy and multi-objective optimization problems of the freight train operation process, scholars at home and abroad have conducted in-depth research and analysis. Ichikawa [2] was the first to study the energy-saving operation strategy of trains, and used the Pontryagin maximum principle to study the optimal control problem of train operation; Scheepmake and Goverde [3] used the Hamiltonian function to deduce that the constant speed and idle point are the keys to energy-saving trains; Yang et al. [4] constructed a lumped energy consumption mechanism model for freight trains, which proved the optimality of constant speed operation in the gentle slope section. Although the above methods have found the optimal operation strategy through rigorous theoretical derivation, they need to make ideal assumptions about trains, lines and other conditions, and do not take into account the nonlinear and complex constraints of the actual operating environment. Cao et al. [5] and Liu et al. [6] consider complex conditions such as trains and lines, build the multi-objective optimization model, and get the operation strategy more in line with the actual situation. However, the multi-objective problem is transformed into a single-objective problem for solving, ignoring the mutual influence among the objectives. To fully embody the essence of multi-objective research, the Pareto principle is usually used to solve such problems. Dullinger et al. [7] designed a multi-objective mixed integer elite genetic algorithm to obtain the Pareto curve of energy consumption and time based on discretization of the circuit; ShangGuan et al. [8] took en-

* Corresponding Author

ergy consumption and time as two optimization goals, and designed an improved multi-objective algorithm combining differential evolution and simulated annealing to solve the problem. This kind of method can get multiple sets of Pareto optimization solutions for decision-makers to choose flexibly, but it does not introduce any preference information, which leads to a wide search range and low efficiency, and may lead to incomplete search and distribution of regional solutions of interest to the final decision-maker. Cheng et al. [9] proposed a multi-objective particle swarm optimization algorithm considering preference information to guide the optimization results to the region expected by the decision-maker; Xiong et al. [10] proposed a multi-objective evolutionary algorithm based on the preference region by dividing the preference region to find the solution that decision-makers are most interested in. Although traditional optimization algorithms such as particle swarms, differential evolution, and NSGA-II have been widely used in the optimization of train operation process, they are prone to fall into local optima and converge slowly. Compared with the above optimization algorithms, the Bald Eagle Search (BES) algorithm has stronger global search ability [11], and can effectively solve various complex optimization problems.

Considering the shortcomings of the above literatures, a multi-objective optimization method for the freight train operation process based on the improved bald eagle search algorithm is proposed in this paper. Firstly, according to the line information, the two-step method is used to find the optimal operation strategy of the freight train, and the multi-objective optimization model of the freight train is established. Secondly, the multi-objective bald eagle search algorithm with better optimization performance is designed by combining preference guidance, improved elite set maintenance mechanism and adaptive Gaussian mutation. In this paper, the HXD1 electric locomotive hauling 54 C80 wagons on the line from “Wandian Station to Xiapingzi Station” in China is used as the experimental object. It is verified by simulation experiments that the proposed improved multi-objective bald eagle search algorithm improves the convergence and distribution of the population, and the optimal target speed curve found can meet the preferences of decision-makers.

2 The Optimal Control Problem of Freight Trains

2.1 Dynamic Model of Freight Train

In this paper, the freight train is taken as the research object. Due to the complex situations such as nonlinearity and multi-marshalling, the traditional single-particle freight train model does not consider the influence of the constraints of the length and coupler force, so there are obvious deviations in the operation of complex lines [12]. In order to obtain a more accurate target speed curve, a freight train multi-particle model is established, and the dynamic differential equation is as follows:

$$\begin{cases} m_1 x_1'' = \mu_t F_t(v) - \mu_b F_b(v) - F_{ch2} - F_{r1}(x,v) \\ \vdots \\ m_i x_i'' = -\mu_b F_b(v) + F_{cqi-1} - F_{chi+1} - F_{ri}(x,v) \\ \vdots \\ m_n x_n'' = -\mu_b F_b(v) - F_{cqn} - F_{rn}(x,v) \end{cases} . \quad \textbf{(1)}$$

Where, $F_t(v)$ and $F_b(v)$ are respectively the traction force and braking force of the freight train, μ_t is the traction coefficient, μ_b is the braking coefficient, $\mu_t \in [0, 1]$, $\mu_b \in [0, 1]$, and $\mu_t \cdot \mu_b = 0$, v is the current speed of the freight train, x is the current position of the freight train, m_i is the weight of the ith freight train, which varies with the on-board load of the train, x_i” is the acceleration of the ith freight train, $F_{cqi\text{-}1}$ is the front coupler force of the ith freight train, F_{cqi+1} is the rear coupler force of the ith freight train, and $F_{ri}(x, v)$ is the total resistance acting on the ith freight train.

The total resistance of freight train is the sum of basic resistance and additional resistance.

$$F_r(x, v) = W_0(v) + W_j(x, v). \quad \textbf{(2)}$$

Where, $W_0(v)$ mainly depends on the speed of freight trains, which can be approximated as a quadratic function of train speed [13]:

$$W_0(v) = \mu_1 + \mu_2 v + \mu_3 v^2. \quad (3)$$

The additional resistance $W_j(x, v)$ is determined by the track characteristics, which mainly include ramps, bends and tunnels, and can be expressed as:

$$W_j(x, v) = w_1(\theta(x)) + w_r(\sigma(x)) + w_1(\tau(x), v). \quad (4)$$

Where, $\theta(x)$, $\sigma(x)$ and $\tau(x)$ are the slope, curve radius and tunnel length along the track respectively [14].

2.2 Operation Strategy of Freight Trains

The optimal operation strategy of trains is composed of four working conditions: maximum traction (MT), constant speed (CS), idle running (IR) and maximum braking (MB) [15-16]. Existing research results show that the optimal operation strategy of trains is MT-CS-IR-MB under the condition of simple lines (such as a straight road). In the case of complex lines such as speed limit, ramp and curve, a two-step method is adopted: firstly, the greedy algorithm is used to select the optimal train working condition sequence, and then the multi-objective optimization algorithm is used to obtain the position of the ideal working condition transition point, so as to obtain the optimal operation strategy of the train. The schematic diagram is shown in Fig. 1.

The starting stage and the final braking stage of the train are usually regarded as a large section respectively without subdivision. For the middle section with higher speed, the line will be divided into k-2 sections according to the line conditions. The maximum traction strategy is adopted at the starting point of the line section. When $v(s_1) > v_l - \Delta v$, the train reaches the s_1 position and starts to change operating conditions. In the middle k-2 sections, the optimal working condition sequence are set according to the algorithm. The maximum braking strategy is adopted at the end of the line section, and the braking position s_{k-1} is obtained by reverse derivation.

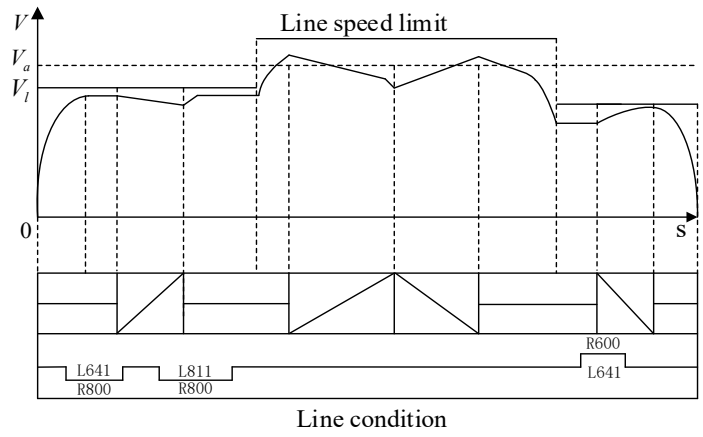

Fig. 1. Schematic diagram of optimal train operation strategy

The sequence of working conditions must meet the following constraints: (1) Traction cannot be followed by braking; (2) The initial working condition is traction and the final working condition is braking; (3) Working conditions should not be changed frequently. The train operation model determines the initial working condition distance sequence $\{s_1, s_2, s_3, \ldots, s_{k-1}, s_k\}$ according to the line division. With the initial working condition distance sequence as the input, the working condition sequence $\{p_1, p_2, p_3, \ldots, p_{k-1}, p_k\}$ is initialized as $\{2, -1, -1, \ldots, -1, -2\}$, where 2, 1, 0, -1, -2 represent traction condition, constant speed condition, idle running condition, condition to be determined and braking condition respectively.

On the premise of ensuring safe operation, this paper takes energy consumption and running time as evaluation indexes of working conditions. To obtain the optimal working condition sequence, the weight summation method is used to design the working condition evaluation index $u_i = a \times e_i + b \times t_i$, where e_i is the energy consumption of the line section, t_i is the running time of the line section, and a and b are the weight coefficients, satisfying $a + b = 1$, where $a = 0.5$, $b = 0.5$. To sum up, the optimization index of working condition sequence is $\sum u_i$, and the smaller the index, the better the working condition sequence.

To obtain the optimal working sequence of freight trains, if exhaustive method is adopted, it is necessary to

conduct 3^{k-2} train operation simulation. In this paper, the greedy algorithm can effectively improve the calculation efficiency, that is, only the current line s_i is considered when determining the working condition p_i. The working condition evaluation indexes $\{u_{i0}, u_{i1}, u_{i2}\}$ corresponding to pi = 0, 1, 2 are calculated in turn, and the working condition corresponding to the minimum evaluation index is taken as the optimal work condition, so as to obtain the optimal working condition sequence of the whole line. In this paper, firstly, the greedy algorithm is used to generate the optimal working condition sequence and obtain the local optimized speed curve, and then the multi-objective optimization algorithm is used to search the position of the ideal working condition transition point and obtain the global optimized speed curve.

3 Multi-objective Optimization and Preference Information of Freight Train Operation

3.1 Multi-Objective Optimization Model of Freight Train

The operation process of freight trains is a complex problem with multiple objectives and constraints, which has some problems such as large energy consumption and long running time caused by unreasonable setting of operating conditions. The optimization of this paper mainly starts from the above problems, and its optimization objectives are energy consumption and running time. Multi-objective optimization is different from the optimization problem with a single objective, in which multiple objectives need to be optimized as much as possible at the same time [17-19].

The energy consumption model of freight trains is:

$$E = \xi_t \int_0^{t_x} P_t(t)dt - \xi_b \int_0^{t_x} P_b(t)dt \quad . \tag{5}$$

Where, E is the energy consumption during the freight train operation, $P_t(t)$ and $P_b(t)$ are the traction power and braking power of the freight train respectively, ξ_t is the transformation factor from electric energy to mechanical energy under the action of traction force, and ξ_b is the transformation factor from mechanical energy to electric energy under the action of braking force.

The running time model [20] is:

$$T = \sum_{i=1}^{n} t_i \quad . \tag{6}$$

Where, T is the total running time, and t_i is the running time of each section of the line.

Meanwhile, in order to ensure the safety of freight train automatic operation and prevent the accidents such as derailment and decoupling, the constraints of freight train operation should be considered.

In order to prevent coupler fracture accidents, the value of coupler force during freight train operation should be less than the value of maximum coupler force recommended by the Academy of Railway Sciences:

$$F_{cqi} \le F_N, F_{chi} \le F_N \quad . \tag{7}$$

Where, F_{cqi} is the front coupler force of the ith freight train F_{chi} is the rear coupler force of the ith freight train, and z is the maximum coupler force of the freight train.

The stationarity of freight trains needs to consider acceleration and speed. In this paper, the change rate of two factors is taken as the adaptive weight. In order to ensure the stationarity of the freight train, the following conditions should be met:

$$J = \sum_{i=1}^{n} w_1 \frac{a_i - a_{i-1}}{dt} + \sum_{i=1}^{n} w_2 \frac{v_i - v_{i-1}}{dt} \le J_N \quad . \tag{8}$$

$$w_1 = \frac{\Delta a_i}{\Delta a_i + \Delta v_i}, w_2 = \frac{\Delta v_i}{\Delta a_i + \Delta v_i} \quad . \tag{9}$$

Where, J is the stationarity index of the freight train, J_N is the maximum stationarity constraint of the freight train, w_1 is the weight of the acceleration change rate of the freight train, and w_2 is the weight of the speed change rate of the freight train.

The constraints of the freight train operation process are as follows:

$$\begin{cases} v(0)=0, v(x_s)=0 \\ 0<v(x_i)\le v_l(x_i) \\ F_{cqi}\le F_N, F_{chi}\le F_N \\ J\le J_N \\ X(0)=0, \Delta x=\left|X_n-D\right|<\Delta x_{\max} \end{cases}. \tag{10}$$

Where, $v(0)$ and $v(x_s)$ are the speed at the starting point and the end point of the running line, $v(x_i)$ is the freight train speed at position x_i, which is required to be lower than the speed limit, $X(0)$ is the starting point of the running line, D is the actual running distance, X_n is the end point of the running line, Δx_{max} is the maximum allowable stopping error, and Δx represents the actual stopping error.

In summary, the multi-objective optimization model of freight train operation process is as follows:

$$\min \ E,T \quad s.t. \begin{cases} v(0)=0, v(x_s)=0 \\ 0<v(x_i)\le v_l(x_i) \\ F_{cqi}\le F_N, F_{chi}\le F_N \\ J\le J_N \\ X(0)=0, \Delta x=\left|X_n-D\right|<\Delta x_{\max} \end{cases}. \tag{11}$$

3.2 Preference Information of Decision-makers

The traditional multi-objective optimization algorithm does not introduce any preference information, which leads to a wide search range and low efficiency, and may lead to the incomplete search and distribution of the regional solution that the final decision-maker interest in. If the preference information of the decision-maker can be combined, the possibility that the preference solution is selected in the iterative process can be changed, and the solution can be driven to move towards the desired region [21].

In this paper, for the practical problem of multi-objective optimization, decision-maker preference is introduced, and the ideal value with sufficient optimization degree of each objective is obtained in advance through the single-objective optimization algorithm and a large number of calculations, and the reference point is obtained accordingly.

For the practical optimization problem with m objectives, the real ideal value cannot be obtained due to the conflict among all objective functions, which needs to be corrected. The calculation formula of the ideal value G_i of the ith objective is as follows:

$$G_i = (\ 1+\varepsilon_i\ ) * \min\ (f_i\ (x)). \tag{12}$$

Where, G_i is the optimization correction coefficient of the ith objective, which is determined by the decision-maker based on the experience of practical application.

According to the set reference point, the vector direction with the origin as the starting point and the reference point as the ending point is constructed as the preference vector direction. The decision-maker can select the optimal solution according to the direction of the preference vector, that is, the solution closest to the preference vector direction is selected as the optimal solution. According to the preference information, the population preference region is divided, and the target space is divided into Preference Region and Non-preference Region, as shown in Fig. 2.

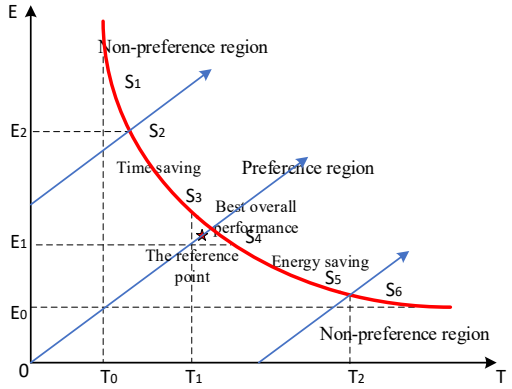

Fig. 2. Schematic diagram of preference region division

In the process of multi-objective optimization, decision-makers often have a certain preference for the optimization target value. The preference of decision-makers for the objective function is set according to the prior information, as shown in Table 1.

Table 1. The preference division of decision-makers

	Perfect	Qualified	Unqualified
Energy consumption (*kJ*)	$[E_0, E_1]$	$[E_1, E_2]$	$[E_2, \infty]$
Running time (*s*)	$[T_0, T_1]$	$[T_1, T_2]$	$[T_2, \infty]$

In this paper, the two objective functions of energy consumption and running time are used to calculate the population preference region. The specific steps are as follows:

Step 1: Divide the sections on the coordinate axis of the objective function according to the level of preference information;

Step 2: Calculate the corresponding points of each boundary point on the front edge: $S_1(T_0, E(T_0))$, $S_2(E_2, T(E_2))$, $S_3(E_1, T(E_1))$, $S_4(T_1, E(T_1))$, $S_5(T_2, E(T_2))$, $S_6(E_0, T(E_0))$;

Step 3: If the following formula is satisfied, it means that there is solution on the Pareto front that satisfy the boundary and the setting is reasonable. According to the preference direction and the preference boundary, the target space can be divided into preference region (S_2, S_5) and non-preference region (∞, S_2) and (S_5, ∞); otherwise, the decision-maker is prompted that the setting is unreasonable and needs to be reset;

$$E_0 < E\,(T_2) < E < E(T_1) < E_2 < E\,(T_0). \tag{13}$$

Step 4: The preference region is further divided into three regions (S_2, S_3), (S_3, S_4) and (S_4, S_5); the first region prefers time-saving, the second region has the best overall performance, and the third region prefers energy saving.

According to the preference information of decision-makers, the target space is divided into preference region and non-preference region, and the solution individuals in the preference region are preferentially selected into the evolution pool, which is conducive to the evolution of population individuals toward the preference region of the decision-maker and provides more solution individuals meeting the requirements for the decision-maker. Meanwhile, the partitioning of the preference region is to set up the preference strategies that satisfy different decision-makers. According to the preference of the decision-maker, different selection probabilities of the optimal position in the preference region were set in the iteration process to drive bald eagle individuals to move towards the most preferred region, which is also convenient for the decision-maker to select the optimal solution in the later stage.

4 Improved Multi-objective Bald Eagle Search Algorithm

4.1 Bald Eagle Search Algorithm

The bald eagle search algorithm is an intelligent optimization algorithm based on the hunting behavior of bald eagle. Individuals in the algorithm are regarded as bald eagle individuals, and the process of finding the optimal solution can be regarded as bald eagle hunting process, which includes three stages: selecting search space, searching selected space, and subducting prey.

In the stage of selecting search space, bald eagle randomly selects a search space close to but different from the previous search space, and updates its position by identifying the best search position and the prior information of random search. Its mathematical model is as follows:

$$X_{i,new} = X_{best} + \alpha * \beta\,(X_{mean} - X_i). \tag{14}$$

Where, α is the parameter that controls the position change, the value range is (1.5, 2), β is the random number between (0, 1), X_{best} is the best search position identified by the current bald eagle, X_{mean} is the average distribution position of the bald eagle after the previous search, and X_i is the position of the ith bald eagle.

After selecting search space, the bald eagle searches the space and updates its position in a spiral flight mode, as shown below:

$$\theta(i) = a * \pi * rand,\ r(i) = \theta(i) + R * rand. \tag{15}$$

$$xr(i) = r(i) * \sin(\theta(i)),\ yr(i) = r(i) * \cos(\theta(i)). \tag{16}$$

$$x(i) = xr(i)/\max(|xr|),\ y(i) = yr(i)/\max(|yr|). \tag{17}$$

$$X_{i,new} = X_i + y(i) * (X_i - X_{i+1}) + x(i) * (X_i - X_{mean}). \tag{18}$$

Where, $\theta(i)$ and $r(i)$ are the polar angle and polar diameter of the spiral equation respectively, a and R are the parameters that control the change of spiral shape, and their value ranges are (0, 5) and (0.5, 2) respectively, *rand* is the random number within (0, 1), and $x(i)$ and $y(i)$ are the bald eagle position in polar coordinates, and their value ranges are both (0, 1).

After searching the space and determining the best position, the bald eagle quickly dives from the best position in the search space to fly towards the target prey. Its mathematical model can be expressed as:

$$\theta(i) = a * \pi * rand,\ r(i) = \theta(i). \tag{19}$$

$$xr(i) = r(i) * \sinh(\theta(i)),\ yr(i) = r(i) * \cosh(\theta(i)). \tag{20}$$

$$xl(i) = xr(i)/\max(|xr|),\ yl(i) = yr(i)/\max(|yr|). \tag{21}$$

$$X_{i,new} = rand * X_{best} + x1(i) * (X_i - c_1 * X_{mean}) + y1(i) * (X_i - c_2 * X_{best}). \tag{22}$$

Where, c_1 and c_2 are the movement intensity of bald eagle to the optimal position and the central position respectively, and their value ranges are both (1, 2).

4.2 Improved Elite Set Maintenance Mechanism

In order to apply the bald eagle search algorithm to the multi-objective optimization problem, the non-dominated sorting idea of non-dominated sorting genetic algorithm-II (NSGA-II) [22] is introduced. After each iteration update, the non-dominated solutions in the population preference region are screened by using the dominance relationship and extended into the elite set. In the updating process, there may be more and more individuals in the elite set population. In order to keep the number of individuals in the elite set population within the upper limit and maintain the diversity of the population, the elite set needs to be tailored.

The traditional elite set maintenance mechanism only considers the distance between the front and back individuals of the individual, but does not consider the bias information of the point, that is, which individual is closer to, and it is difficult to improve its distribution quickly. In order to quickly improve the distribution of elite sets, this paper proposes an improved elite set maintenance mechanism. The specific steps are as follows:

Step 1: Take the maximum and minimum values of each objective function as the boundary, divide the objective function section into k-2 sections (k is the storage number of elite set), and count the number of non-dominant individuals in each section;

Step 2: Then the uniform distribution variance D (f_i) of different sections on each objective function is calculated according to Eq. (23), and the maximum objective function of D (f_i) is taken as the partition standard;

$$D(f_i) = \frac{1}{k-2}\left(\sum_{i=0}^{k-2} x_i - \bar{x}\right) . \tag{23}$$

Where, $\bar{x}$ is the average number in the total section;

Step 3: Select the section with the densest distribution of individuals, and calculate the density h (θ) between individuals by the cosine distance formula;

$$h(\theta) = cos(\theta) = \frac{\sum_{i=1}^{m}(a_i - b_i)}{\sqrt{\sum_{i=1}^{m} a_i^2} * \sqrt{\sum_{i=1}^{m} b_i^2}} . \tag{24}$$

Step 4: Select the two or more individuals with the closest density, and delete one individual at a time through the crowding distance formula;

$$D_j = \sum_{i=1}^{m} \frac{f_{j+1}^i - f_{j-1}^i}{f_{max}^i - f_{min}^i} . \tag{25}$$

Where, m is the number of the objective function, f_{max}^i and f_{min}^i are the maximum and minimum fitness values on the ith objective respectively, f_{j+1}^i and f_{j-1}^i are the fitness values of the front and back individuals of individual j on the ith objective respectively, and D_j is the crowding degree of the jth individual.

Step 5: Check whether the number of elite sets p is greater than the storage number of elite sets k, and if p is greater than k, turning to step 1, otherwise, ending the operation.

As can be seen from Fig. 3, when the crowding distance calculation formula is used alone, the crowding distance at point B is smaller than that at point D, so individual B should be deleted, but it is obvious that individual D is more crowded. This method does not consider the bias information of this point and cannot accurately reflect the crowding degree of individuals. Therefore, this paper first calculates the uniform distribution variance of the two objective function sections, where D (f_1) > D (f_2), then divides the function f_1 section, selects the individuals B, C, D, E and F in the section with the densest individual distribution, selects the two densest individuals D and E by the cosine distance formula, and then removes the individual D by the crowding distance formula. Through the above steps, the distribution of elite set can be rapidly improved.

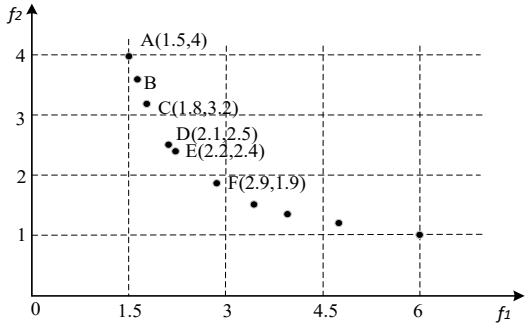

Fig. 3. Improved elite set maintenance mechanism

4.3 Flow Chart of IMOBES

The bald eagle search algorithm (BES) performs optimization based on the current optimal position to make it have certain directional guidance, which is conducive to its accelerated convergence and global optimization. However, this will make the evolution of the bald eagle population too dependent on the optimal position, which will result in the loss of diversity and is not conducive to global convergence. In order to solve the problem that multi-objective algorithm falls into local optimal solution, adaptive Gaussian variation is added in the position update. During the iterative process of the algorithm, each dimension of each individual decision variable has a certain probability of Gaussian variation with the standard deviation of σ^2. The adaptive strategy is introduced. With the increase of the number of iterations, the variation range of the population gradually decreases, which is larger in the early iteration period and smaller in the late iteration period. Its mathematical model is shown in Eqs. (26) ~ (28) [23]:

$$X_{i,j}{}' = \begin{cases} lb_{i,j}, GM(X_{i,j},\sigma^2) < lb_j \\ ub_{i,j}, GM(X_{i,j},\sigma^2) > ub_j \\ GM(X_{i,j},\sigma^2), otherwise \end{cases} . \tag{26}$$

$$\sigma^2 = \sigma_0{}^2 e^{-k/G_{max}} . \tag{27}$$

$$\sigma_0{}^2 = \frac{ub_{i,j} - lb_{i,j}}{20} . \tag{28}$$

Where, $lb_{i,j}$ and $ub_{i,j}$ are the minimum and maximum values of the j-th code of the i-th individual respectively, $\sigma_0{}^2$ is the standard deviation, $GM(X_{i,j}, \sigma^2)$ is a random number generated by the normal distribution, and its mean value and standard deviation are $X_{i,j}$ and σ^2 respectively.

Based on the above reasons, the multi-objective bald eagle search algorithm designed in this paper adopts the evolution method of adopts the evolution mode of combining bald eagle population update with adaptive Gaussian mutation, and uses the preference information given in this paper to enhance the rationality of evolution. Combined with the above sections, the flow chart of the improved multi-objective bald eagle search algorithm proposed in this paper is shown in Fig. 4.

Considering the convergence and diversity of the optimization algorithm, the temporary population composed of the elite set and some individuals of the bald eagle population is adopted as the temporary population of adaptive Gauss variation. As can be seen from Fig. 4, based on the original Pareto dominance relationship, this paper selects the non-dominant solution according to the decision-maker's preference information. Meanwhile, in the iterative process, guided by the preference information, different selection probabilities of the optimal position in the preference area are set, which drives the bald eagle individual to move towards the most preferred region, so that it is easy to find the optimal solution that is more satisfactory to the decision-maker. The preference direction vector is constructed according to the preference reference points set by the decision-maker, and the solution closest to the preference direction vector on the Pareto front is selected as the output preference solution.

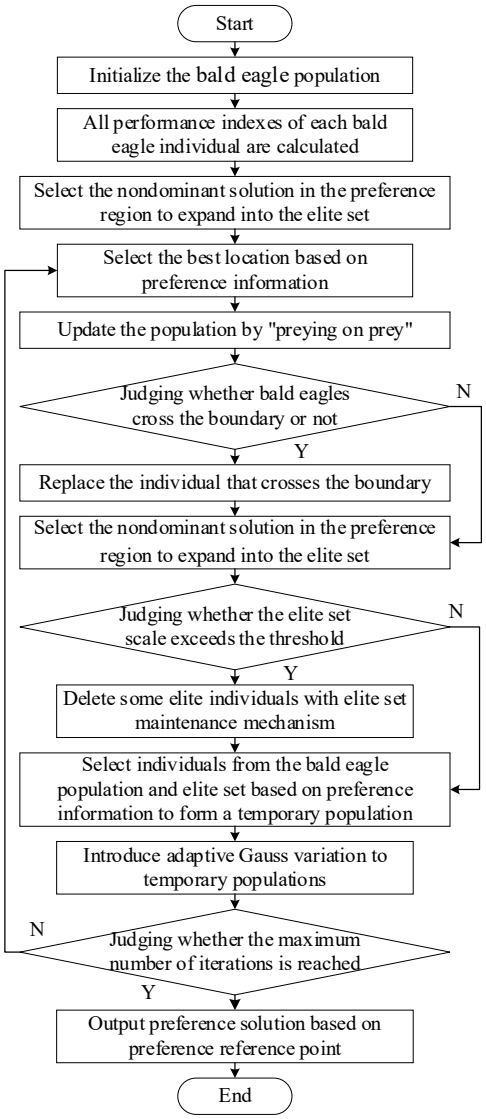

Fig. 4. The flow chart of the improved multi-objective bald eagle search algorithm

5 Simulation Experiment and Analysis

5.1 Data on the Operation of Freight Trains

In this paper, the HXD1 electric locomotive hauling 54 C80 wagons on the line from "Wandian Station to Xiapingzi Station" is used as the experimental object. Simulation experiments are conducted based on actual line and operation data to verify the effectiveness of the proposed method. In this section, the speed limit of the general line is 80 *km*/*h*, and the speed limit of the multi-curve section is 70 *km*/*h*. Part of the line data of "Wandian Station to Xiapingzi Station" is shown in Fig. 5, and the basic attributes of the freight train are shown in Table 2.

Table 2. Basic parameters of freight trains

Parameter name	Parameter characteristics
Formation plan	1 Locomotive+54 wagons
Self-weight of locomotive and wagon (*t*)	184, 20
Length of locomotive and wagon *(m)*	35.222, 12.2
wagon loading weight (*t*)	80
Unit basic resistance of locomotive (*N/kN*)	$1.2+0.0065v+0.000279v^2$
Unit basic resistance of wagon (*N/kN*)	$0.92+0.0048v+0.000125v^2$
Maximum running speed (*km/h*)	80

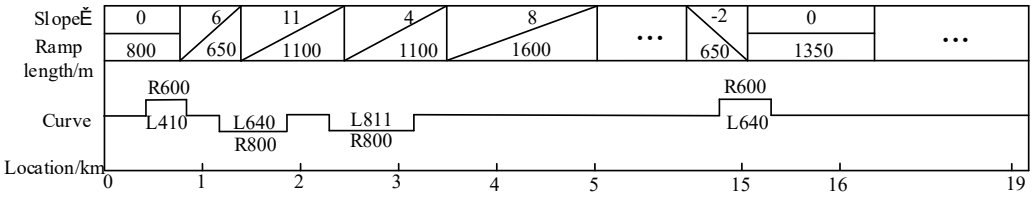

Fig. 5. Partial line data from Wandian station to Xiapingzi station

5.2 Experimental Parameter Setting

The parameters of the improved multi-objective bald eagle search (IMOBES) algorithm are set as follows: the size of the bald eagle population is 100, the size of the elite set is 100, the size of the temporary population is 100, and the number of iterations k_{max} is 100. The parameters of the freight train operating environment experiment are set as follows: the maximum couple force constraint is $F_N \leq 1000\ kN$, the stationarity constraint is $J_N \leq 55$. After the single-objective optimization and the prior calculation of equation (15), the preference reference points for energy saving, time saving and optimal comprehensive performance are set as (4750, 1235), (5180, 1120) and (4950, 1182) respectively (energy consumption unit is $10^3 \cdot kJ$, time unit is s). Referring to the relevant provisions of international standard ISO 2631-1 [24] and the actual operation of freight trains, the division of train performance indicators is set, as shown in Table 3. The above parameter settings consider the parameter characteristics and the results of several experimental simulations.

Table 3. Specific division of decision-makers' preferences

	Perfect	Qualified	Unqualified
Energy consumption ($10^3 \cdot kJ$)	[4600, 4850]	[4850, 5300]	[5300, ∞]
Running time (s)	[1080, 1150]	[1150, 1280]	[1280, ∞]

5.3 Experimental Results and Analysis

Under the above experimental conditions, IMOBES algorithm, Multi-objective Bald Eagle Search (MOBES) algorithm, Multi-objective Particle Swarm Optimization (MOPSO) algorithm and NSGA-II are respectively used to optimize the operation process of the freight train. Fig. 6 shows the distribution of frontier solutions using the IMOBES algorithm, MOBES algorithm, MOPSO algorithm and NSGA-II. As can be seen from the figure, the IMOBES algorithm can ensure that the solution sets are in the preference region and meet the goals of energy saving and time saving, and the Pareto frontier solution is closer to the inner side with better convergence. Overall, the energy consumption calculated by it is significantly lower and the time is shorter. In addition, compared with MOBES, MOPSO and NSGA-II, the Pareto frontier solutions obtained by the MOBES algorithm are densely and uniformly distributed, showing better distribution, and the number of Pareto frontier solutions in the preference region is more. However, the solutions obtained by the other three algorithms have solutions that do not conform to actual engineering applications, and the gaps between adjacent solutions are not uniform, which needs to be filled to increase the diversity of solutions.

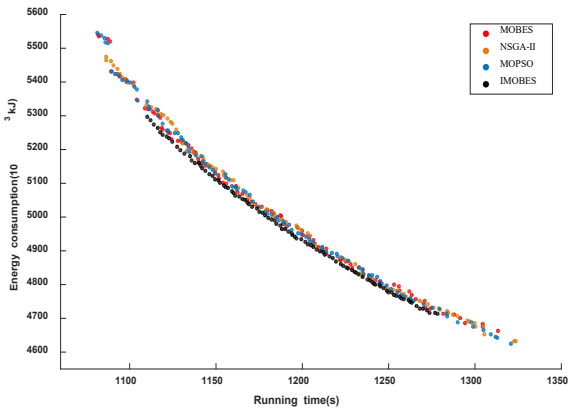

Fig. 6. Pareto frontier distribution of four algorithms

As can be seen from Fig. 7 and Fig. 8, compared with MOBES, MOPSO and NSGA-II, the computational efficiency of the IMOBES algorithm is greatly improved, and its global convergence is faster in the preference region. The IMOBES algorithm rapidly converges to the optimal solution in the preference region, while other algorithms converge more slowly, and some of the optimal solutions of convergence do not conform to the engineering practice.

The proposed algorithm not only has a good optimization effect, but also meets the expectation of decision-makers in terms of energy consumption and running time. According to the preference reference point set by the decision-maker, the solution closest to the preference direction vector on the Pareto front is selected as the output preference solution. As can be seen from Table 4, the IMOBES algorithm (preference 1) finds the optimal solution with energy saving, the IMOBES algorithm (preference 2) finds the optimal solution with less running time, and the IMOBES algorithm (preference 3) finds the optimal solution with the best overall performance.

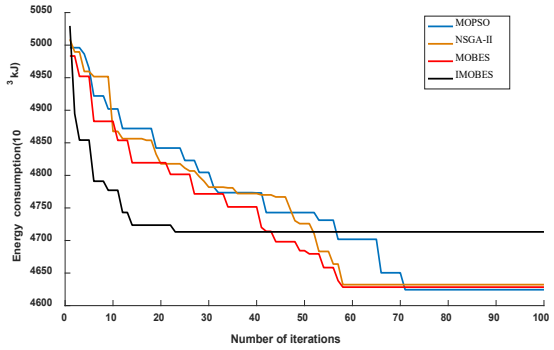

Fig. 7. Iterative convergence curve of energy consumption

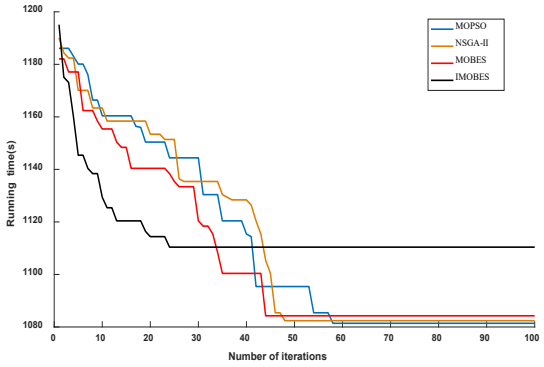

Fig. 8. Iterative convergence curve for running time

Table 4. Optimization results of different preferences

Preferred target	Energy consumption ($10^3 \cdot kJ$)	Running time (s)
IMOBES (Preference 1)	4768.51	1253
IMOBES (Preference 2)	5222.16	1124
IMOBES (Preference 3)	4965.74	1188

The corresponding speed-distance curve of freight train with energy saving, time saving and best overall performance is shown in Fig. 9, and the operating condition is shown in Fig. 10. Where, “2” represents the traction condition sequence, “1” represents the cruising condition sequence, “0” represents the idling condition sequence, and “-2” represents the braking condition sequence.

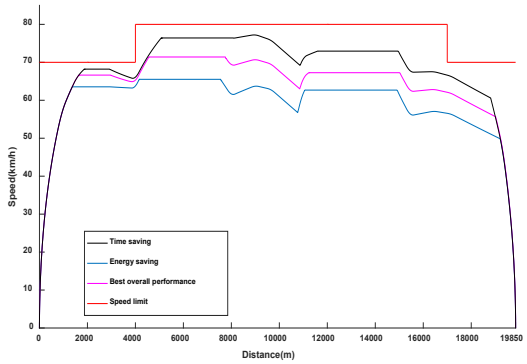

Fig. 9. Speed-distance curves of freight trains with three strategies

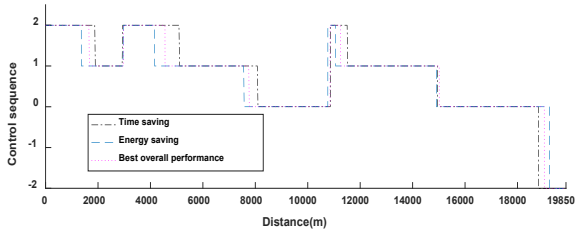

Fig. 10. Control sequence of freight train with three strategies

In this paper, the solution with the best overall performance is selected as the optimized solution. The comparison data before and after optimization is shown in Table 5.

Table 5. Comparison data before and after optimization

	Energy consumption ($10^3 \cdot kJ$)	Running time (s)
Before optimization	5713.93	1087
After optimization	4965.74	1188

The energy consumption of freight train operation before optimization is 5713.93 × 103 kJ, and the running time is 1087s. The optimized train makes reasonable use of cruise and idle running conditions, increases the running time of the train to a certain extent, and greatly reduces the energy consumption of the train operation, which reduces 13.09% compared with the energy consumption before optimization, and can realize the energy saving optimization of freight train operation. Fig. 11 and Fig. 12 respectively show the distance-velocity curve and control sequence curve before and after optimization.

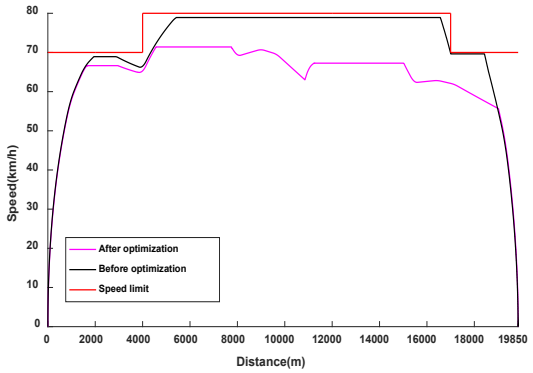

Fig. 11. Speed-distance curve of freight train before and after optimization

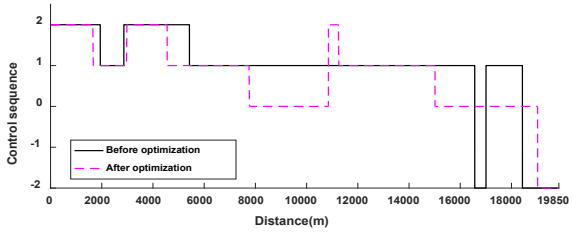

Fig. 12. Freight train control sequence before and after optimization

In order to reflect the advantages of the designed method, for the same line conditions, the professional simulation software (*Train Traction Calculation and Simulation System* 1.0) developed by *Shijiazhuang Tiedao University* is used in this paper for comparative simulation, and the results are shown in Fig. 13.

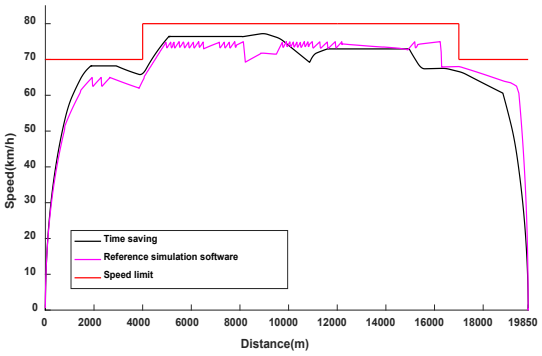

Fig. 13. Comparison between the method in this paper and the reference simulation software

As can be seen from the Fig. 13, the driving strategy in this paper (taking the driving strategy with time saving as an example) is that in the low-speed limit section of 0~3*km*, the train speed is first increased to about 68.2*km* by traction condition and then maintain at a uniform speed. Then entering the large ascending ramp section of 3~4*km*, the vehicle speed still decreases under the maximum traction condition. After passing through the low-speed limit section, in the ramp section of 4~7.8*km*, the train speed is increased to 76.4*km*/*h* by traction condition, and then the train keeps the uniform speed. In the middle ramp sections, the alternating operating mode of idling, traction and cruising is adopted to ensure that the train speed is between 60 and 80*km*/*h*, while making full use of the descending ramp section for energy saving. At 15.3~18.8*km*, the idling condition is adopted to reduce the train speed and prepare to stop. After 18.8*km*, the braking condition is adopted to reduce the train speed and stop the train.

As for the referenced simulation software, the cruising condition is not considered in the operation process. The train speed is lower than the speed limit by alternating traction and idling conditions. The freight train operating conditions change frequently, and the operation strategy is extremely unreasonable. In the low-speed limit section of 0~3*km*, the train speed is first increased to about 65*km* by traction condition, and then the alternating operation conditions of traction and idling condition are adopted to keep the train speed at about 65*km*. Then entering the large ascending ramp section of 3~4*km*, the vehicle speed still decreases under the maximum traction condition. After passing through the low-speed limit section, in the ramp section of 4~7.8*km*, the train speed is increased to 75*km*/*h* by traction condition. Then the train speed is kept at about 75*km*/*h* by alternating traction and idling operating conditions. The train's maximum traction time is long and the energy consumption is more. In addition, the method does not use idling condition to reduce the speed in advance in the descending ramp section at about 7.8*km* and 15.3*km*, but uses braking condition to prevent the speed exceeding the speed limit in the descending ramp section. In order to reduce energy consumption, the train usually uses braking only for the purpose of stopping, and the operation strategy is unreasonable. The energy consumption of the method used in the simulation software is $6036.96\times10^3 kJ$ and the running time is 1241*s*. Its energy consumption is $814.8\times10^3 kJ$ more than the method in this paper, and its running time is 117*s* longer than the method in this paper.

6 Conclusion

The multi-objective optimization of freight train operation is a complex optimization and decision problem. The freight train runs on a long line and the line conditions are complex and changeable. This paper adopts a two-step method to determine the optimal operation strategy of the freight train, and designs a multi-objective bald eagle search algorithm with better optimization performance, which is applied to the optimization of the freight train running process. Through the simulation experiment, the following conclusions are obtained:

1) The freight train operation strategy selected by the two-step method is in line with the actual operating conditions and meets the requirements of energy-saving and time-saving. The simulation results show that compared with the referenced simulation software, the proposed method has less energy consumption and shorter running time.

2) By introducing the preference of the decision-maker, the possibility of the preference solution being selected in the iteration process is changed, and the solution is driven to move towards the desired region. Meanwhile, the elite set maintenance mechanism is improved and adaptive Gaussian variation is introduced. Compared with other algorithms, the Pareto front of the IMOBES algorithm has better convergence and distribution.

3) For the Pareto frontier solution, combined with preference information, the optimal operation scheme that meets the requirements of decision-makers can be selected, which improves the practicability of engineering applications.

7 Acknowledgement

This work was supported by the National Natural Science Foundation of China (61572416), Hunan Province Natural Science Zhuzhou United Foundation (2020JJ6009), Key Laboratory Open Project Fund of State Heavy Duty AC Drive Electric Locomotive Systems Integration.

References

[1] H. Tong, J. Peng, Y. Zhang, T. Fang, J. Zhang, Z. Men, Y. Liu, L. Wu, T. Wang, F. Ren, H. Xu, W. Wang, Z. Du, H. Mao, Environmental benefit analysis of “road-to-rail” policy in China based on a railway tunnel measurement, Journal of Cleaner Production 316(2021) 128227.

[2] K. Ichikawa, Application of optimization theory for bounded state variable problems to the operation of train, Bulletin of JSME 11(47)(1968) 857-865.

[3] G.M. Scheepmaker, R.M. Goverde, The interplay between energy-efficient train control and scheduled running time supplements, Journal of Rail Transport Planning & Management 5(4)(2015) 225-239.

[4] J. Yang, L.M. Jia, S.F. Lu, Z.Y. Li, Energy-efficient operation of electric freight trains-part I: Speed Profile Optimization, Journal of the China Railway Society 38(4)(2016) 22-31.

[5] Y. Cao, Z.C. Wang, F. Liu, P. Li, G. Xie, Bio-inspired speed curve optimization and sliding mode tracking control for subway trains, IEEE Transactions on Vehicular Technology 68(7)(2019) 6331-6342.

[6] K.W. Liu, X.C. Wang, Z.H. Qu, Research on multi-objective optimization and control algorithms for automatic train operation, Energies 12(20)(2019) 3842.

[7] C. Dullinger, W. Struckl, M. Kozek, Simulation-based multi-objective system optimization of train traction systems, Simulation Modelling Practice and Theory 72(2017) 104-117.

[8] W. ShangGuan, X.H. Yan, B.G. Cai, J. Wang, Multiobjective optimization for train speed trajectory in CTCS high-speed railway with hybrid evolutionary algorithm, IEEE Transactions on Intelligent Transportation Systems 16(4)(2015) 2215-2225.

[9] S. Cheng, M.Y. Chen, P.J. Fleming, Improved multi-objective particle swarm optimization with preference strategy for optimal DG integration into the distribution system, Neurocomputing 148(2015) 23-29.

[10]M. Xiong, W. Xiong, C. Liu, A hybrid many-objective evolutionary algorithm with region preference for decision makers, IEEE Access 7(2019) 117699-117715.

[11]H.A. Alsattar, A.A. Zaidan, B.B. Zaidan, Novel meta-heuristic bald eagle search optimisation algorithm, Artificial Intelligence Review 53(3)(2020) 2237-2264.

[12]J.J. Meng, X.Q. Chen, R.X. Xu, Y.L. Zhang, T.Z. Wei, X.Q. Jiang, Traction Calculation Analysis and Simulation of Urban Rail Train on Multi-particle Model, Journal of System Simulation 27(3)(2015) 603-608.

[13]Y. Song, W. Song, A novel dual speed-curve optimization based approach for energy-saving operation of high-speed trains, IEEE Transactions on Intelligent Transportation Systems 17(6)(2016) 1564-1575.

[14]L. Zhang, X. Zhuan, Optimal operation of heavy-haul trains equipped with electronically controlled pneumatic brake systems using model predictive control methodology, IEEE Transactions on Control Systems Technology 22(1)(2014) 13-22.

[15]A. Albrecht, P. Howlett, P. Pudney, X. Vu, P. Zhou, The key principles of optimal train control—Part 1: Formulation of the model, strategies of optimal type, evolutionary lines, location of optimal switching points, Transportation Research Part B: Methodological 94(2016) 482-508.
[16]A. Albrecht, P. Howlett, P. Pudney, X. Vu, P. Zhou, The key principles of optimal train control—Part 2: Existence of an optimal strategy, the local energy minimization principle, uniqueness, computational techniques, Transportation Research Part B: Methodological 94(2016) 509-538.
[17]M. Barraza, E. Bojórquez, E. Fernández-González, A. Reyes-Salazar, Multi-objective optimization of structural steel buildings under earthquake loads using NSGA-II and PSO, KSCE Journal of Civil Engineering 21(2)(2017) 488-500.
[18]F. Bre, V.D. Fachinotti, A computational multi-objective optimization method to improve energy efficiency and thermal comfort in dwellings, Energy and Buildings 154(2017) 283-294.
[19]C. Steenkamp, A.P. Engelbrecht, A scalability study of the multi-guide particle swarm optimization algorithm to many-objectives, Swarm and Evolutionary Computation 66(2021) 100943.
[20]J. Cao, B. Liu, Research on simulation for energy-saving operation of high-speed trains based on two-stage optimization, Journal of Railway Science and Engineering 15(4)(2018) 821-828.
[21]Y. Hu, J. Zheng, J. Zou, S. Jiang, S. Yang, Dynamic multi-objective optimization algorithm based decomposition and preference, Information Sciences 571(2021) 175-190.
[22]K. Deb, A. Pratap, S. Agarwal, T. Meyarivan, A fast and elitist multiobjective genetic algorithm: NSGA-II, IEEE transactions on evolutionary computation 6(2)(2002) 182-197.
[23]H. Fang, A. Zhou, H. Zhang, Information fusion in offspring generation: A case study in DE and EDA, Swarm and Evolutionary computation 42(2018) 99-108.
[24]International Organization for Standardization, Mechanical vibration and Shock—evaluation of human exposure to whole-body vibration—part 1: General requirements, ISO 2631-1, 1997.